Lawrence Berkeley National Laboratory
Recent Work

Title
The ultraviolet photochemistry of phenylacetylene and the enthalpy of formation of 1,3,5-hexatriyne

Permalink
https://escholarship.org/uc/item/50c3r2j0

Journal
Journal of the American Chemical Society, 123(4)

Author
Sorkhabi, Osman

Publication Date
2000-05-01

ERNEST ORLANDO LAWRENCE
BERKELEY NATIONAL LABORATORY

BERKELEY LAB

The Ultraviolet Photochemistry of Phenylacetylene and the Enthalpy of Formation of 1,3,5-Hexatriyne

Osman Sorkhabi, Fei Qi, Abbas H. Rizvi,
and Arthur G. Suits

Chemical Sciences Division

May 2000

DISCLAIMER

DISCLAIMER

The Ultraviolet Photochemistry of Phenylacetylene and the Enthalpy of Formation of 1,3,5-Hexatriyne

Osman Sorkhabi, Fei Qi, Abbas H. Rizvi,
and Arthur G. Suits

Chemical Sciences Division
Ernest Orlando Lawrence Berkeley National Laboratory
University of California
Berkeley, California 94720

May 2000

The ultraviolet photochemistry of phenylacetylene and the enthalpy of formation of 1,3,5-Hexatriyne

Osman Sorkhabi, Fei Qi, Abbas H. Rizvi, and Arthur G. Suits*

Chemical Sciences Division, Ernest Orlando Lawrence Berkeley National Laboratory, Berkeley, CA 94720

Abstract: The ultraviolet photochemistry of phenylacetylene (PA) was studied in a molecular beam at 193 nm. The only primary photofragments characterized were HCCH (acetylene) and C_6H_4. The most likely isomers of C_6H_4 were assigned as either (E)-3-hexene-1,5-diyne or (Z)-3-hexene-1,5-diyne on the basis of energetic considerations. Some of the C_6H_4 molecules were found to decompose to 1,3,5-hexatriyne and molecular hydrogen. An enthalpy of formation of $\Delta H_f \leq 154 \pm 4$ kcal mol^{-1} was determined for 1,3,5-hexatriyne from the energetic threshold for this process. This experimentally determined value agrees well with our *ab initio* calculations performed at the *G2* level of theory. Angular distribution measurements for the HCCH + C_6H_4 channel yielded an isotropic distribution and was attributed to a long-lived intermediate and ground state dissociation. An exhaustive search yielded no evidence for the phenyl + ethynyl or the atomic hydrogen elimination channels even though these were observed in the pyrolytic studies of PA [Hofmann, J.; Zimmermann, G.; Guthier, K.; Hebgen, P.; Homann, K. H. *Liebigs Ann.* **1995**, *631*, 1995; Guthier, K.; Hebgen, P.; Hofmann, K. H.; Zimmermann, G. *Liebigs Ann.* **1995**, *637*, 1995].

1

Introduction

Phenylacetylene (PA) is an aromatic molecule with an unsaturated side group and is commonly used as a precursor for the synthesis of the polymer polyphenylacetylene.[1-6] Like other cyclic aromatic hydrocarbons, PA is believed to be an important contributor to the formation of polycyclic aromatic hydrocarbons (PAH) in combustion and in interstellar space.[7-13] In the initial pyrolytic studies of PA, acetylene and benzene were identified as end products and it was postulated that further reactions involving them led to cyclization reactions and PAH formation.[7-9] Subsequently, Hofmann, *et al.* carried out a detailed analysis of the reaction products from the pyrolysis of PA.[10] PAHs with up to four rings were observed and their results confirmed that pyrolysis of PA could indeed lead to PAH formation. In a collaborative study with Hofmann, *et al.*, Zimmermann and co-workers identified several transient products for the unimolecular dissociation of PA, among these were the free radicals phenyl, phenylvinyl, and *ortho-*, *meta-*, and *para-*ethynylphenyl.[11] Assuming that these transient species are primary products, these observations indicate the presence of several atomic hydrogen elimination channels. Pyrolytic studies, however, provide limited and at times ambiguous results for the primary processes due to the presence of multiple collisions and subsequent competition with secondary and tertiary chemical reactions. It is therefore desirable to unambiguously determine the identity of the primary products from the ground state unimolecular dissociation of PA.

We have carried out an ultraviolet (UV) photochemical investigation of PA using photofragment translational spectroscopy (PTS) on the Chemical Dynamics Beamline at the Advanced Light Source in Berkeley. This investigation is part of an ongoing effort to

understand the UV photochemistry of large polyatomic aromatic molecules.[14,15] In such systems, dissociation occurs mostly via the ground state potential energy surface (PES) following internal conversion from the initially prepared excited electronic state.[14-16] This allows for the study of the unimolecular dissociation on the ground state PES under *collision free* conditions. Therefore, the photochemistry of large polyatomic molecules using PTS is a powerful technique for the determination of the primary processes in the unimolecular dissociation of these molecules in an *unambiguous* manner.

Several vibronic bands of PA have been observed in the UV and are attributed to excitation of the ring electrons with vibrational coupling to the C-C stretch of the acetylenic moiety.[17,18] These features were also revealed in the theoretical investigation of Narayanan, *et al.*[19] The UV spectroscopy and vibrational structure of the ground and excited states of PA have been well established yet little is known about its photochemistry.[19-23] We have carried out an investigation of the photodissociation of PA at 193 nm to gain more insight into the primary processes involved and to extend our study of polyatomic aromatic molecules to PA. At 193 nm, the vibronic transitions involve those of the $D\ ^1A_1 \leftarrow A\ ^1A_1$ or $E\ ^1A_1 \leftarrow A\ ^1A_1$ systems.[17] At this wavelength, we identified one primary photochemical pathway:

$$C_6H_5\text{-CCH} + h\nu_{193} \rightarrow C_6H_4 + HCCH \qquad \Delta H_{rxn} = -37.9 \text{ kcal mol}^{-1} \qquad (1).$$

The UV photochemistry of PA is surprisingly simple. Reaction (1) produces two closed shell molecules – acetylene (HCCH) and (E)-3-hexene-1,5-diyne or (Z)-3-hexene-1,5-diyne (C_6H_4). The amount of energy available in this process is sufficient to induce a secondary reaction:

$$C_6H_4^* \qquad \rightarrow \qquad C_6H_2 + H_2 \qquad (2),$$
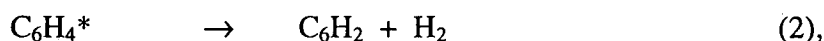
Where $C_6H_4^*$ is internally excited C_6H_4 and C_6H_2 has been characterized as 1,3,5-hexatriyne which is also referred to as triacetylene in the literature. From the energetic threshold for reaction (2), an upper limit of 154 ± 4 kcal mol^{-1} for the enthalpy of formation of 1,3,5-hexatriyne was estimated. Quantum *ab initio* calculations at the *G2* level of theory agree well with this value. Figure 1 shows the energy diagram for the 193 nm photodissociation of PA. In recent years, much effort has gone into the determination of the thermochemistry and heats of formations of diacetylene, triacetylene, and other unsaturated hydrocarbons.[24-28] Our result for the heat of formation of triacetylene is the first experimentally determined value for this quantity.

Experimental Section

All experiments were conducted at beamline 9.0.2.1 of the Advanced Light Source using a rotatable source molecular beam machine which was described in detail in an earlier publication.[29] This machine can be used to study reactive scattering[30,31] and photodissociation dynamics.[14,32] In the present photodissociation experiment, helium was bubbled through a PA sample at room temperature. At this temperature and a total pressure of 800 Torr, a 1% molecular beam of PA/He was generated. This mixture was fed through a pulsed valve (General Valve) and expanded from a nozzle heated to ~100°C in a differentially pumped source region and into the main chamber. The pressure in the source chamber was maintained at 2×10^{-4} Torr with the beam on. The molecular beam was collimated with two skimmers (0.03" and 0.02") and its velocity and speed ratio were either measured by using a chopper wheel or a laser hole-burning

method. Both methods gave consistent results and typical values for the velocity and speed ratio were found to be 1870 ± 40 m s^{-1} and 11 ± 2, respectively.

The photolysis laser was an ArF excimer (193 nm, Lambda Physik LPX 220i), focused to a spot of size 2x4 mm and aligned perpendicular to the plane containing the molecular beam and detector axis, on the axis of rotation of the molecular beam source. Photofragments entering the triply differentially pumped detector region (9×10^{-11} Torr) were photoionized 15.2 cm from the interaction region using tunable synchrotron radiation. The characteristics of the light source are discussed in detail elsewhere and include an intensity of 10^{16} photons/sec (quasi-continuous), an energy bandwidth of 2.2%, and a cross section in the probe region of 0.2x0.1 mm.[33] The tunability of the light source allowed for selective ionization of products and very low background counts. The photoionized products were mass selected by using a quadrupole mass filter and the ions were counted with a Daly ion counter.[34] Time-of-flight of the products were measured with a multichannel scaler (EG&G Ortec Turbo MCS). The bin width for the MCS was fixed at 1 μsec for the measurements reported here. Timing sequences for the laser, pulsed valve, and the MCS were maintained by a digital delay generator (Stanford Research Systems, Inc. Model 535). Eight quartz plates fixed at Brewster's angle were used for the polarization measurements to give $87\pm5\%$ polarized light. To rotate the angle of polarization with respect to the detector axis, a half wave plate was used (Karl Lambrecht). Phenylacetylene (98%) was obtained from Aldrich and used without further purification.

Ab initio calculations were performed with either the Q-Chem software package[35] run on a LINUX based 500 MHz personal computer or the Gaussian 98 software

package[36] run on the National Energy Research Scientific Computing Center's Cray supercomputer parallel vector processor cluster (http://www.nersc.gov). Calculations were carried out at several levels of theory for the ΔH_f of acetylene, diacetylene, and triacetylene. Of all the calculations performed, the G2 results were found to be the most accurate and the results will be provided in the next section.
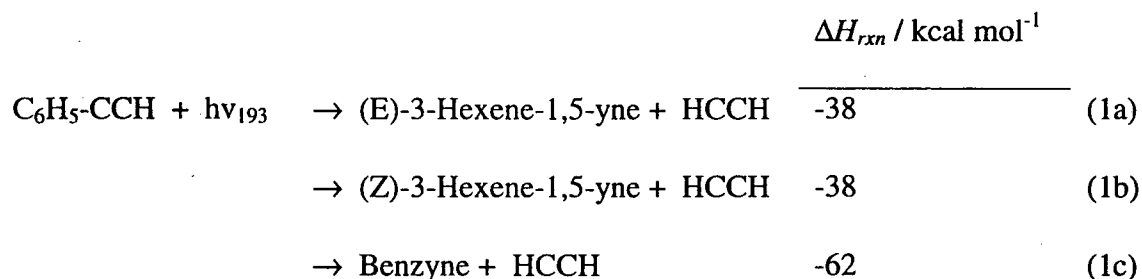
Results and Discussion

Signal was observed for m/e 26, 74, and 76 corresponding to HCCH, C_6H_2, and C_6H_4, respectively. The signal for each of these fragments was measured as a function of laser pulse energy and data was recorded in the single photon regime. In the presentation of the data, the open circles represent the experimental data and the solid lines represent the best fit to the data. An energy diagram for the photodissociation of PA at 193 nm is provided in Fig. 1.

Photochemistry. The measured TOF spectra for m/e 26 (HCCH) at laboratory angles of 15° and 30° are shown in Fig. 2. To convert from the laboratory-frame velocity distribution (such as those in Fig. 2) to the center-of-mass velocity distributions, $P(E)$, the forward convolution method was applied to the data.[37,38] The best fits to the C_2H_2 data - solid lines in Fig. 2 – resulted in the $P(E)$ shown in Fig 4a. This distribution has an average translational energy of 12 kcal mol^{-1} and extends out to a maximum value of about 40 kcal mol^{-1}. If C_2H_2 and C_6H_4 are momentum matched photofragments, then the same $P(E)$ should fit both data sets. Attempts were made to fit the C_6H_4 data with the distribution of Fig 4a, however, the slow C_6H_4 fragments could not be accounted for (refer to Fig. 3). To get the best fit for the C_6H_4 fragment, the slower portion of the $P(E)$

of Fig 4a had to be removed. This depletion of the distribution suggests the presence of a secondary dissociation process since the slower fragments will have enough internal energy to induce this process [see reaction (2)]. In fact, the difference of 4a and 4b results in a distribution which fits the $C_6H_2 + H_2$ experimental data reasonably well. However, a better fit was obtained when the fast edge of the distribution was adjusted (see Fig. 5). The modified center-of-mass distribution is shown in Fig. 4c. These results indicate that the primary C_6H_4 fragments formed with sufficient internal energy decompose to C_6H_2 and H_2. The energetics of this process will be discussed in more detail in the next section.

The probable isomers for C_6H_4 are (E)-3-hexene-1,5-yne, (Z)-3-hexene-1,5-yne, and benzyne. Therefore, reaction (1) may be rewritten as:

$$\Delta H_{rxn} \text{ / kcal mol}^{-1}$$

C_6H_5-CCH + hv_{193}	→ (E)-3-Hexene-1,5-yne + HCCH	-38	(1a)
	→ (Z)-3-Hexene-1,5-yne + HCCH	-38	(1b)
	→ Benzyne + HCCH	-62	(1c)

Typically, the center-of-mass translational energy distribution of photofragments extends out to the maximum available energy.[16,32] The distribution which best fits the C_6H_4 data extends out to about 40 kcal mol^{-1} and matches well with the available energy for reactions (1a) and (1b). Given this fact alone, one can likely assign the identity of C_6H_4 to (E)-3-hexene-1,5-yne and (Z)-3-hexene-1,5-yne. For certain molecules, measurement of their photoionization efficiency (PIE) spectra can further help in assigning the identity of a given molecule.[14,32] PIE spectra may be conveniently measured by tuning the VUV undulator radiation while monitoring the integrated ion signal. The PIE spectrum of

C_6H_4 was measured and the ionization threshold was found to occur at about 9 eV. Ionization potentials (IP) for (E)-3-hexene-1,5-yne, (Z)-3-hexene-1,5-yne, and benzyne are 9.07 ± 0.02 eV,[39] 9.10 ± 0.02 eV,[39] and 9.03 ± 0.05,[40] respectively. Since the IPs of these isomers are so close in value, however, we are unable to verify our assignment of the identity of the C_6H_4 fragment solely based from the PIE data. Figure 6 shows the PIE spectrum for the C_6H_2 fragment. The most likely structure for C_6H_2 is 1,3,5-hexatriyne since the threshold of ionization from its PIE curve matches well with the reported IP of 9.50 ± 0.02 eV for 1,3,5-hexatriyne.[41] Spectroscopic characterization of the products may be necessary to establish their identities with greater certainty. The spectroscopy of open chain and cyclic unsaturated hydrocarbons are well known, thus, either I.R., visible, and/or UV spectroscopic techniques may be employed to measure and characterize their identity.[42-49]

Angular distribution measurements for reaction (1) were made and the anisotropy parameter, β, was determined as described in a previous publication.[14] A β parameter of nearly zero was obtained and most likely implies a lifetime for the intermediate at least as long as several rotational periods. A β parameter of zero, singlet products, and an apparent statistical product distribution all indicate that the dissociation may occur via the ground state surface after internal conversion for the 193 nm photodissociation of PA. The UV excitation of PA involves a $\pi \rightarrow \pi*$ transition and the delocalized electronic system extends to the acetylenic moiety.[17-19] Since this transition involves the excitation of an electron from a bonding to an anti-bonding orbital, a decrease in the C-C bond order of the conjugated system will lead to a geometry change in the excited state. This geometry change could enhance the probability of internal conversion to high lying

vibrational levels of the ground electronic state of PA (due to a larger Franck-Condon overlap integral). Our data indicates the presence of internally excited C_6H_4 which could arise from the dissociation of vibrationally excited, "hot", PA. Although a detailed mechanism of the dissociation is beyond the scope of the present study, the data suggests the following mechanism. After excitation of PA by the 193 nm photon to the $D\ ^1A_1$ or $E\ ^1A_1$ states, internal conversion to the ground electronic state ($A\ ^1A_1$) produces "hot" PA. Subsequently, the "hot" PA decomposes to vibrationally excited C_6H_4 and HCCH [see reaction (1)]. This process would require the opening of the ring and is consistent with characterization of C_6H_4 as either (E)- and (Z)-3-hexene-1,5-diyne as discussed above. Some of the C_6H_4 products have sufficient internal energy to undergo secondary dissociation [see reaction (2)] to produce 1,3,5-Hexatriyne and molecular hydrogen.

Ground state unimolecular dissociation of PA has been studied recently by pyrolysis and the results may be compared with the results obtained here.[7-11] Frank and co-workers and Hopf, *et al.* identified acetylene and benzene as the end products in their pyrolytic studies.[7-9] More recently, PAHs were also identified as end products.[10] In a subsequent study, Guthier, *et al.* reported the observation of several free radicals including phenyl, phenylvinyl, and *ortho-*, *meta-*, and *para-*ethynylphenyl with phenyl being the major radical product.[11] The observation of phenyl indicates the presence of the phenyl + ethynyl channel as well as several H atom elimination channels if these radicals are generated from primary processes. As mentioned above, photodissociation of PA most likely occurs on the ground state surface. If so, then phenyl as well as phenylvinyl, and *ortho-*, *meta-*, and *para-*ethynylphenyl should also be observed in our PTS measurements. However, an exhaustive search yielded no evidence for the phenyl +

ethynyl or the atomic hydrogen elimination channels. Guthier, *et al.* used a radical scavenger method to characterize the radicals generated in their pyrolytic studies of PA. Although this is a powerful method for the characterization of the free radicals produced, it does not distinguish whether or not these free radicals are primary products. Given that these results do not concur with our PTS results indicates that these free radicals may not be primary products.

Thermochemistry. It was mentioned above that the secondary dissociation of C_6H_4 [reaction (2)] occurred as a result of the large amount of internal energy released in this fragment. The distributions of Fig 4b and 4c clearly demonstrate this. A striking feature of these distributions is the sharp energetic cutoff for the secondary dissociation. This cutoff indicates that the $C_6H_2 + H_2$ products have negligible internal energies and provides an opportunity for the determination of the enthalpy of formation for the C_6H_2 fragment. Table 1 lists the relevant reactions along with their energetics. The enthalpy of reaction for step A in Table 1 was calculated using values of ΔH_f obtained from literature. The enthalpy of reaction for step B in Table 1 (i.e. $C_6H_4^* \rightarrow C_6H_2 + H_2$) was determined from the distribution of Fig 4c and is given by the difference between E_{av} (37.9 kcal mol^{-1}) and E_{cutoff} (12.8 kcal mol^{-1}) where E_{av} is the available energy [see reaction (1)] and E_{cutoff} is the cutoff energy for the secondary decomposition [i.e. maximum translational energy in the distribution of Fig. 4c]. The sum of steps A and B in Table 1 gives the overall reaction, $C_6H_5C_2H \rightarrow C_6H_2 + HCCH + H_2$, and its ΔH_{rxn} is simply the sum of the ΔH_{rxn} for steps A and B. Using 73.3 and 54.4 kcal mol^{-1} for the ΔH_f of $C_6H_5C_2H$ and HCCH, respectively, and 135.3 kcal mol^{-1} for the ΔH_{rxn} for step C, an upper limit of 154 ± 4 kcal mol^{-1} was calculated for the heat of formation of C_6H_2

(1,3,5-hexatriyne). The error in this value was determined by checking the sensitivity of the fit in Fig. 5 to E_{cutoff}.

Theoretical calculations were employed to give us a better handle on the thermochemistry described above. Single point calculations were performed at the MP2/6-311G(d,p), CISD/6-311G(d,p), B3LYP/6-311G(d,p), and $G2$ levels of theory for acetylene, 1,3-butadiyne (diacetylene), and 1,3,5-hexatriyne (triacetylene). Enthalpies of formation were calculated using these values according the atomization[50-55] and formation reaction procedures[54-57]. These procedures gave satisfactory results only for acetylene. Therefore, an alternative procedure was employed. Using the following reaction

$$nC_2H_2 \rightarrow C_{2n}H_2 + n/2 \ H_2$$
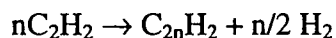
where n = 2 for 1,3-butadiyne and n = 3 for 1,3,5-hexatriyne, we can write

$$\Delta H_{rxn} = n/2 \ \Delta H_f (H_2) + \Delta H_f (C_{2n}H_2) - n \ \Delta H_f (C_2H_2).$$

Solving for ΔH_f ($C_{2n}H_2$) and substituting $\{G2(C_{2n}H_2) + n/2 \ G2(H_2) - nG2(C_2H_2)\}$ for ΔH_{rxn}, we get

$$\Delta H_f (C_{2n}H_2) = G2(C_{2n}H_2) + n/2 \ G2(H_2) - nG2(C_2H_2) + n \ \Delta H_f (C_2H_2).$$

The enthalpies of formation for 1,3-butadiyne and 1,3,5-hexatriyne calculated using this procedure agree well with experimental values. These results along with experimental values are summarized in Table 2.

The value of 154 ± 4 kcal mol^{-1} should be taken as an upper limit for the ΔH_f of 1,3,5-hexatriyne due to the possible presence of a barrier for the reverse reaction. The reverse reaction could involve the addition of molecular hydrogen across a triple bond - a process which typically requires an energy barrier of about 2 eV (46 kcal mol^{-1}).[58,59]

However, the data suggests that 141 kcal mol^{-1} may be near the energy minimum of the products since little energy is released into product translational energy (see Fig 4c). This presents an apparent dilemma in which the threshold energy of 141 kcal mol^{-1} may be near the energy minimum of the products yet an energy barrier is expected for the reverse reaction (please refer to Fig. 1). Conversely, a three-center dissociation involving a 3,4-hydride shift in either (E) or (Z)-3-hexene-1,5-yne will have a significantly lower barrier. The barrier for the reverse reaction will be much lower than 2 eV if such a hydride shift is involved. Hydride shifts in ethylene and polyenes are greatly facilitated by the torsional motion about the C=C bond.[60,61] The (E)/(Z)-3-hexene-1,5-yne molecules have sufficient internal energy (as evident from the distribution of Fig. 4b) and it is conceivable that some of this energy will be in the torsional vibrations of the 4,5-C=C bond. This motion should greatly facilitate a 4,5-hydride shift and cause reaction (2) to proceed via a nearly barrier-less path and, thus, nullify the apparent dilemma mentioned above.

Conclusions

This paper presents the study of the photodissociation dynamics of phenylacetylene (PA) at a wavelength of 193 nm using photofragment translational spectroscopy (with tunable VUV as the ionization method). The results presented are part of an ongoing effort at the Chemical Dynamics Beamline of the Advanced Light Source to unravel the photodissociation dynamics of cyclic-polyatomic molecules. For such systems, dissociation via the ground state potential energy surface following internal conversion is the dominant dissociative pathway. A key aspect of these studies is the

determination of the primary processes in such events. The 193 nm dissociation of PA was found to yield only one primary channel - C_6H_4 + C_2H_2. The primary product fragments were characterized as (E)- and/or (Z)-3-hexene-1,5-diyne and acetylene, respectively. The (E)- and/or (Z)-3-hexene-1,5-diyne molecules, with sufficient energy, were found to undergo *secondary* dissociation to produce C_6H_2 + H_2. The C_6H_2 fragment was characterized as 1,3,5-hexatriyne by measuring its photoion yield spectrum. A heat of formation (ΔH_f) of 154 ± 4 kcal mol^{-1} was determined for 1,3,5-hexatriyne and this value agrees well with the results of our *ab initio* calculations.

* Corresponding author: AGSuits@lbl.gov

References

1. Simionescu, C. I.; Percec, V. *Prog. Polym. Sci.* **1982**, *8*, 133.

2. Masuda, T.; Higashimura, T. *Adv. Polym. Sci.* **1987**, *81*, 121.

3. Furlani, A.; Licoccia, S.; Russo, M. V.; Camus, A.; Marisch, N. *J. Polym. Sci. Polym. Chem. Ed.* **1986**, *24*, 991.

4. Shivasubramaniam, V.; Sundararajan, G. *J. Molec. Catalysis* **1991**, *65*, 205.

5. Lachmann, G.; Duplessis, J. A. K.; Dutoit, C. J. *J. Molec. Catalysis* **1990**, *58*, 143.

6. Zhang, J.; Fu, K. *Polym. Bulletin* **1994**, *32*, 63.

7. Hopf, H.; Musso, H. *Angew. Chem.* **1969**, *81*, 704.

8. Hopf, H.; Musso, H. *Angew Chem. Int. Ed.* **1969**, *8*, 680.

9. Herzler, J.; Frank, P. *Ber. Bunsenges. Phys. Chem.* **1992**, *96*, 1333.

10. Hofmann, J.; Zimmermann, G.; Guthier, K.; Hebgen, P.; Homann, K. H. *Liebigs. Ann.* **1995**, *1995*, 631.

11. Guthier, K.; Hebgen, P.; Homann, K. H; Hofmann, J.; Zimmermann, G. *Liebigs. Ann.* **1995**, *1995*, 637.

12. Frenklach, M.; Feigelson, E. D. *Astrophys. J.* **1989**, *341*, 372.

13. Goeres, A.; Keller, R.; Sedlmary, E.; Gail, H. P. *Polycyclic Aromatic Compounds* **1996**, *8*, 129.

14. Sorkhabi, O.; Qei, F.; Rizvi, A. H.; Suits, A. G. *J. Chem. Phys.* **1999**, *111*, 100.

15. Qei, F.; Sorkhabi, O.; Rizvi, A. H.; Suits, A. G. *J. Phys. Chem.* **1999**, *103*, 8351.

16. Blank, D. A.; North, S. W.; Lee, Y. T. *Chem. Phys.* **1994**, *187*, 35.

17. Swiderek, P.; Gootz, B.; Winterling, H. *Chem. Phys. Lett.* **1998**, *285*, 246.

18. Leopold, D. G.; Hemley, R. J; Vaida, V.; Roebber, J. L. *J. Chem. Phys.* **1981**, *75*, 4758.

19. Narayanan, K.; Chang, G. C.; Shieh, K. C.; Tung, C. C.; Tzeng, W. B. *Spectroch. Acta A* **1996**, *52*, 1703.

20. King W.; So, S. P. *J. Mol. Spectrosc.* **1971**, *38*, 543.

21. Singh, H.; Laposa, J. D. *J. Luminesc.* **1972**, *5*, 32.

22. Powers, D. E.; Hopkins, J. B.; Smalley, R. E. *J. Chem. Phys.* **1981**, *74*, 5971.

23. Chia, L.; Goodman, L. *J. Chem. Phys.* **1982**, *76*, 4745.

24. Ball, D. W. *J. Mol. Struct. Theochem.* **1997**, *417*, 107.

25. Nicholaides, A.; Radom, L. *Mol. Phys.* **1996**, *88*, 759.

26. Schulman, J. M.; Disch, R. L. *J. Mol. Struct. Theochem.* **1992**, *91*, 173.

27. Curtiss, L. A.; Raghavachari, K.; Redfern, P. S.; Rassolov, V.; Pople, J. A. *J. Chem. Phys.* **1998**, *109*, 7764.

28. Kiefer, J. H.; Sidhu, S. S.; Kern, R. D.; Xie, K.; Chen, H.; Harding, L. B. *Combust. Sci. Technol.* **1992**, *82*, 101.

29. Yang, X.; Lin, J.; Lee, Y. T.; Blank, D. A.; Suits, A. G.; Wodke, A. M. *Rev. Sci. Instrum.* **1997**, *68*, 3317.

30. Hemmi, N.; Suits, A. G. *J. Chem. Phys.* **1998**, *109*, 5338.

31. Blank, D. A.; Hemmi, N.; Suits, A. G.; Lee, Y. T. *Chem. Phys.* **1998**, *231*, 261.

32. Sun, W. Z.; Yokoyama, K.; Robinson, J. C.; Suits, A. G.; Neumark, D. M. *J. Chem. Phys.* **1999**, *110*, 4363.

33. Heimann, P.A.; Koike, M.; Hsu, C. W.; Evans, M.; Ng, C. Y.; Blank, D. A.; Yang, X. M.; Flaim, C.; Suits, A. G.; Padmore, H. A.; Lee, Y. T. *Rev. Sci. Instrum.* **1997**, *68*, 1945.

34. Lee, Y. T.; McDonald, J. D.; LeBreton, P. R.; Herschbach, D. R. *Rev. Sci. Instrum.* **1969**, *40*, 1402.

35. *Q-Chem.* White, C. A.; Kong, J.; Maurice, D. R.; Adams, T. R.; Baker, J.; Challacombe, M.; Schwegler, E.; Dombroski, J. P.; Ochsenfeld, C.; Oumi, M.; Furlani, T. R.; Florian, J.; Adamson, R. D.; Nair, N.; Lee, A. M.; Ishikawa, N.; Graham, R. L.; Warshel, A.; Johnson, B. G.; Gill, P. M. W.; Head-Gordon, M. *Q-Chem*, Version 1.2, Q-Chem, Inc., Pittsburgh, PA, 1998.

36. *Gaussian 98, Revision A.5*, Frisch, M. J.; Trucks, G. W.; Schlegel, H. B.; Scuseria, G. E.; Robb, M. A.; Cheeseman, J. R.; Zakrzewski, V. G.; Montgomery, Jr., J. A.; Stratmann, R. E.; Burant, J. C.; Dapprich, S.; Millam, J. M.; Daniels, A. D.; Kudin, K. N.; Strain, M. C.; Farkas, O.; Tomasi, J.; Barone, V.; Cossi, M.; Cammi, R.; Mennucci, B.; Pomelli, C.; Adamo, C.; Clifford, S.; Ochterski, J.; Petersson, G. A.; Ayala, P. Y.; Cui, Q.; Morokuma, K.; Malick, D. K.; Rabuck, A. D.; Raghavachari, K.; Foresman, J. B.; Cioslowski, J.; Ortiz, J. V.; Stefanov, B. B.; Liu, G.; Liashenko, A.; Piskorz, P.; Komaromi, I.; Gomperts, R.; Martin, R. L.; Fox, D. J.; Keith, T.; Al-Laham, M. A.; Peng, C. Y.; Nanayakkara, A.; Gonzalez, C.; Challacombe, M.; Gill, P. M. W.; Johnson, B.; Chen, W.; Wong, M. W.; Andres, J. L.; Gonzalez, C.; Head-Gordon, M.; Replogle, E. S.; Pople, J. A. Gaussian, Inc., Pittsburgh PA, 1998.

37. Wodtke, A. M.; Ph.D. Thesis, University of California at Berkeley, 1986.

38. Zhao, X.; Ph.D. Thesis, University of California at Berkeley, 1988.

39. Roth, W. R.; Adamczak, O.; Breuckmann, R.; Lennartz, H. W.; Boese, R. *Chem. Ber.* **1991**, *124*, 2499.

40. Zhang, X.; Chen, P. *J. Am. Chem. Soc.* **1992**, *114*, 3147.

41. Bieri, G.; Burger, F.; Heilbronner, E.; Maier, J. P. *Helv. Chim. Acta* **1977**, *60*, 2213.

42. Hass, S.; Winnewisser, G.; Yamada, K M. T.; Matsumura, K. *J. Mol. Spectrosc.* **1994**, *167*, 176.

43. Delpech, C.; Guillemin, J. C.; Paillous, P.; Khlifi, M. *Spectroc. Acta A* **1994**, *50*, 1095.

44. Radziszewski, J. G.; Hess, B. A.; Zahradnik, R. J. *J. Am. Chem. Soc.* **1992**, *114*, 52 and references therein.

45. Nam, H. H.; Leroi, G. E. *J. Mol. Struct.* **1987**, *157*, 301 and references therein.

46. Wenthold, P.G.; Squires, R. R.; Lineberger, W. C. *J. Am. Chem. Soc.* **1998**, *120*, 5279.

47. Marquardt, R.; Sander, W.; Kraka, E. *Angew. Chem.* **1996**, *108*, 825.

48. Arrington, C. A.; Ramos, C.; Robinson, A. D.; Zwier, T. S. *J. Phys. Chem. A* **1999**, *103*, 1294.

49. Arrington, C. A.; Ramos, C.; Robinson, A. D.; Zwier, T. S *J. Phys. Chem. A* **1998**, *102*, 3315.

50. Pople J. A.; Curtiss, L. A. *J. Chem. Phys.* **1991**, 95, 4385.

51. Curtiss, L. A.; Nobes, R. H.; Pople, J. A.; Radom, L. *J. Chem. Phys.* **1992**, *97*, 6766.

52. Wong M. W.; Radom, L. *J. Am. Chem. Soc.* **1993**, *115*, 1507.

53. Glukhovtsev, M. N.; Pross, A.; Radom, L. *J. Phys. Chem.* **1996**, *100*, 3498.

54. Schlege H. B.; Skancke, A. *J. Am. Chem. Soc.* **1993**, *115*, 7465.

55. Nicolaides, A.; Rauk, A.; Glukhovtsev, M. N.; Radom, L. *J. Phys. Chem.* **1996**, *100*, 17460.

56. Armstrong, D. A.; Rauk, A.; Yu, D. *J. Am. Chem. Soc.* **1993**, *115*, 666.

57. Yu, D.; Rauk, A.; Armstrong, D. A. *Can. J. Chem.* **1994**, *72*, 471.

58. Chang, A. H. H.; Mebel, A. M.; Yang, X. M.; Lin, S. H.; Lee, Y. T. *J. Chem. Phys.* **1998**, *109*, 2748.

59. Lin, J. J.; Hwang, D. W.; Lee, Y. T.; Yang, X. *J. Chem. Phys.* **1998**, *109*, 2979.

60. Ohmine, I *J. Chem. Phys.* **1985**, *83*, 2348.

61. Freund, L.; Klessinger, M. *Int. J. Quant. Chem.* **1998**, *70*, 1023.

62. Chase, M. W., Jr., *J. Phys. Chem. Ref. Data* **1998**, *9*, 1-1951.

63. Kiefer, J. H.; Sidhu, S. S.; Kern, R. D.; Xie, K.; Chen, H.; Harding, L. B. *Combust. Sci. Technol.* **1992**, *82*, 101.

Figure captions

Figure 1. Energy diagram for the photodissociation of phenylacetylene at a wavelength of 193nm. Two possible primary pathways leading to m/e 76 + m/e 26 momentum matched fragments are shown. The path leading to HCCH + A or B is higher in energy than the one leading to HCCH + C. In this figure, A, B, and C refer to (Z)-3-hexene-1,5-diyne, (E)-3-hexene-1,5-diyne, and benzyne, respectively. The energetics were calculated using literature values for ΔH_f of A, B, C, and acetylene. The energetic threshold for the secondary process (i.e. the one leading to C_6H_2 + HCCH + H_2) was determined from the experimentally measured center-of-mass translational energy distribution of Fig. 4. The energetic cutoff for the secondary decomposition is also shown along with the $P(E)$ of Fig. 4.

Figure 2. Time-of-flight spectra of m/e 26 measured at laboratory angles of 15 and 30 degrees. Both of spectra were measured with an ionization photon energy of 12.5 eV. Open circles represent the experimental data and the solid line represents the forward convolution fit to the data.

Figure 3. Time-of-flight spectra of m/e 76 measured at laboratory angles of 10, 15 and 20 degrees. These spectra were measured with a photon ionization energy of 10 eV. A MgF_2 optical filter was used to filter all photons with energies of 11.2 eV or higher. Open circles represent the experimental data and the solid line represents the forward convolution fit to the data.

Figure 4. The fits shown in Figs. 2 and 3 resulted in the center-of-mass translational energy distributions, $P(E)$, shown here. (a) The $P(E)$ used to fit m/e 26 (HCCH) fragment. (b) This panel clearly shows that some of the distribution is missing. In fact, the subtraction of (b) from (a) gives the residual shown in (c). This residual fits the data in Fig. 5 quite well. Refer to the text for more details.

Figure 5. Time-of-flight spectrum of m/e 74 (C_6H_2) measured at a laboratory angle of 5 degrees. The residual distribution of Fig. 4c is momentum matched with the data shown here. Refer to the text for more details.

Figure 6. To get the photoionization efficiency spectrum for m/e 74, integrated ion signal at m/e 74 was measured as a function of the photon energy. Note that the ionization onset of this curve occurs at about 9 eV and matches well with the ionization potential for 1,3,5-hexatriene (i.e. 9.5 eV).
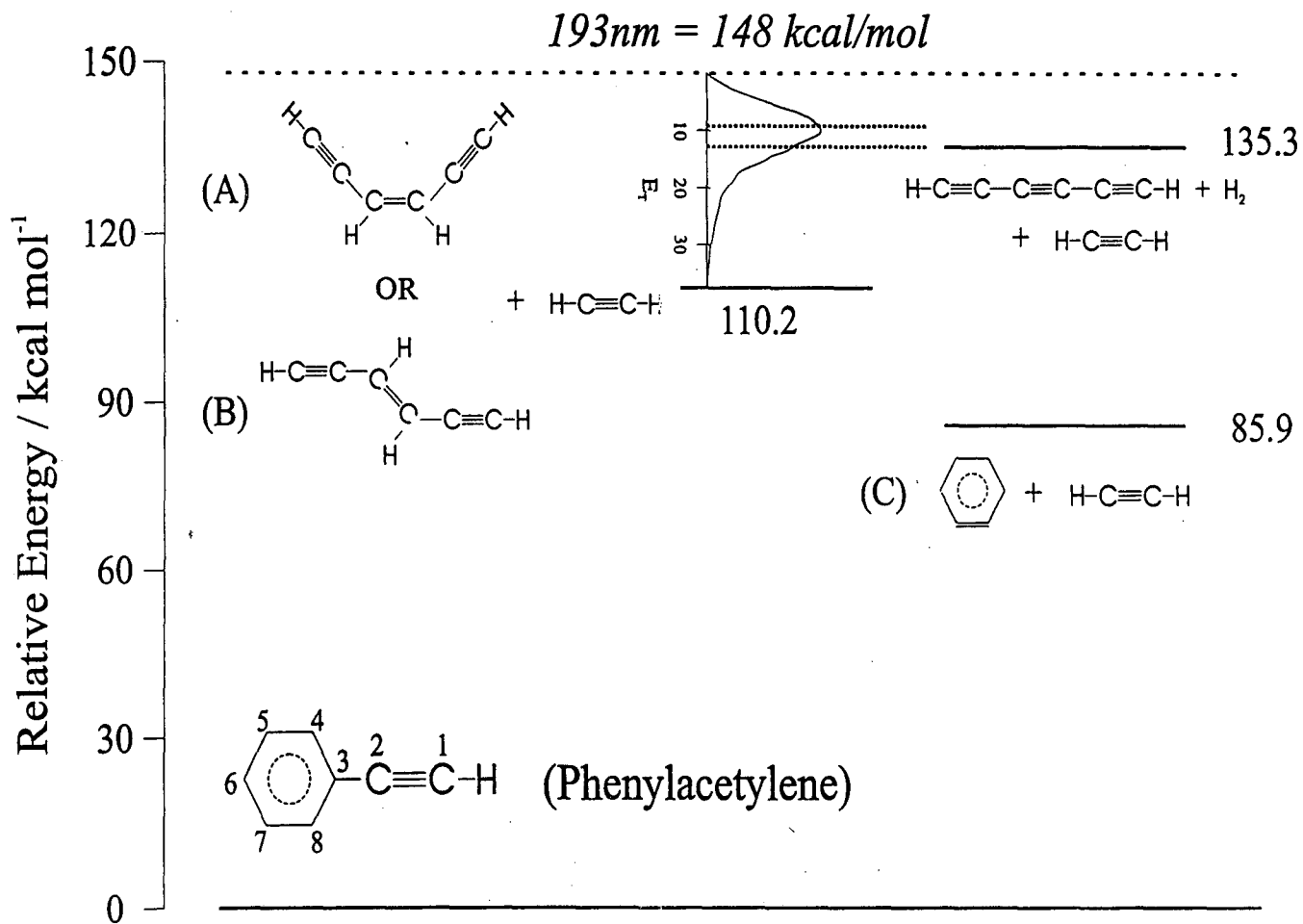
Table 1. Relevant reactions and their energetics. For reaction (B), ΔH_{rxn} was determined from the available energy (E_{av}) and the energetic cutoff for the secondary decomposition (E_{cutoff}). Refer to the text for more details
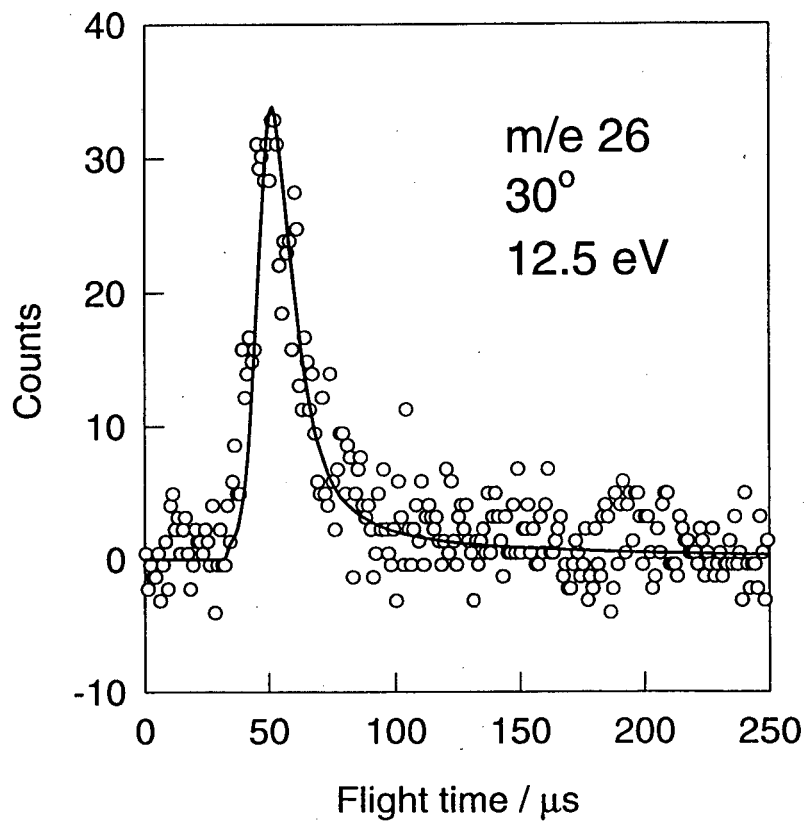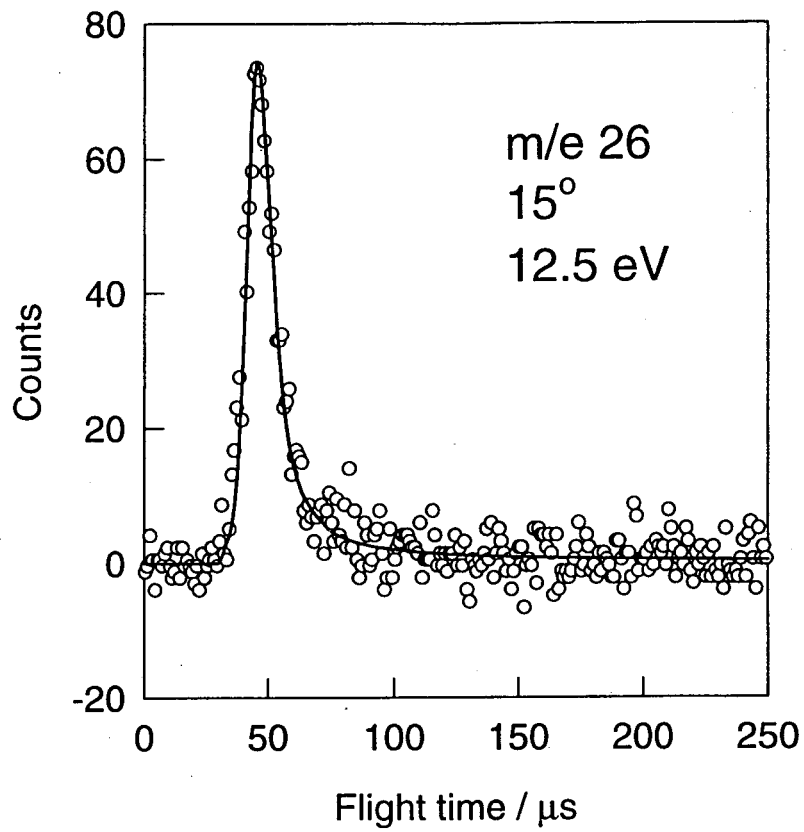
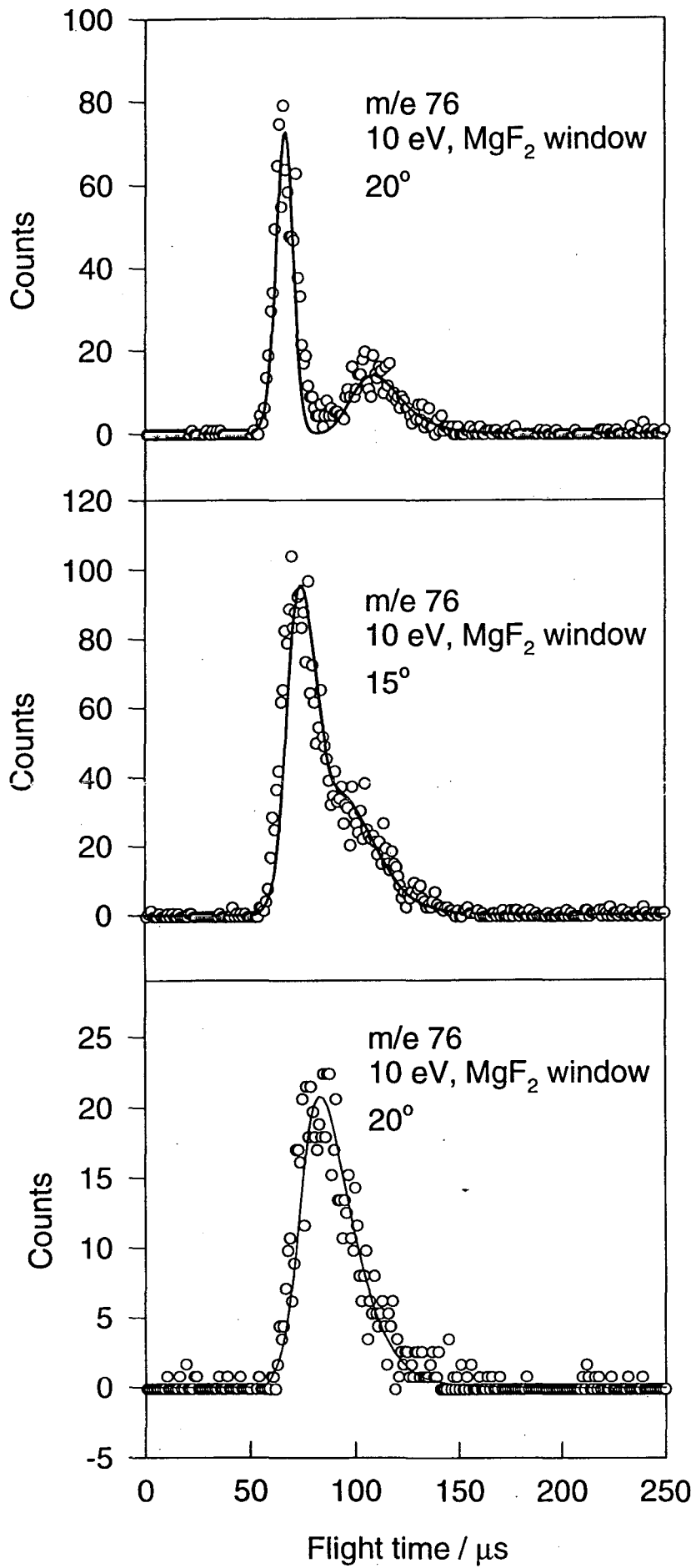|		ΔH_{rxn} / kcal mol^{-1}	
$C_6H_5\text{-}C_2H$	$\rightarrow C_6H_4^* + C_2H_2$	110.2	(A)
$C_6H_4^*$	$\rightarrow C_6H_2 + H_2$	$E_{av} - E_{cutoff} = 25.1$	(B)
$C_6H_5\text{-}C_2H$	$\rightarrow C_6H_2 + C_2H_2 + H_2$	135.3	(C)

Table 2. A comparison of the experimental and calculated ΔH_f (0 Kelvin) for acetylene, 1,3-butadiyne (diacetylene), and 1,3,5-hexatriyne (triacetylene)
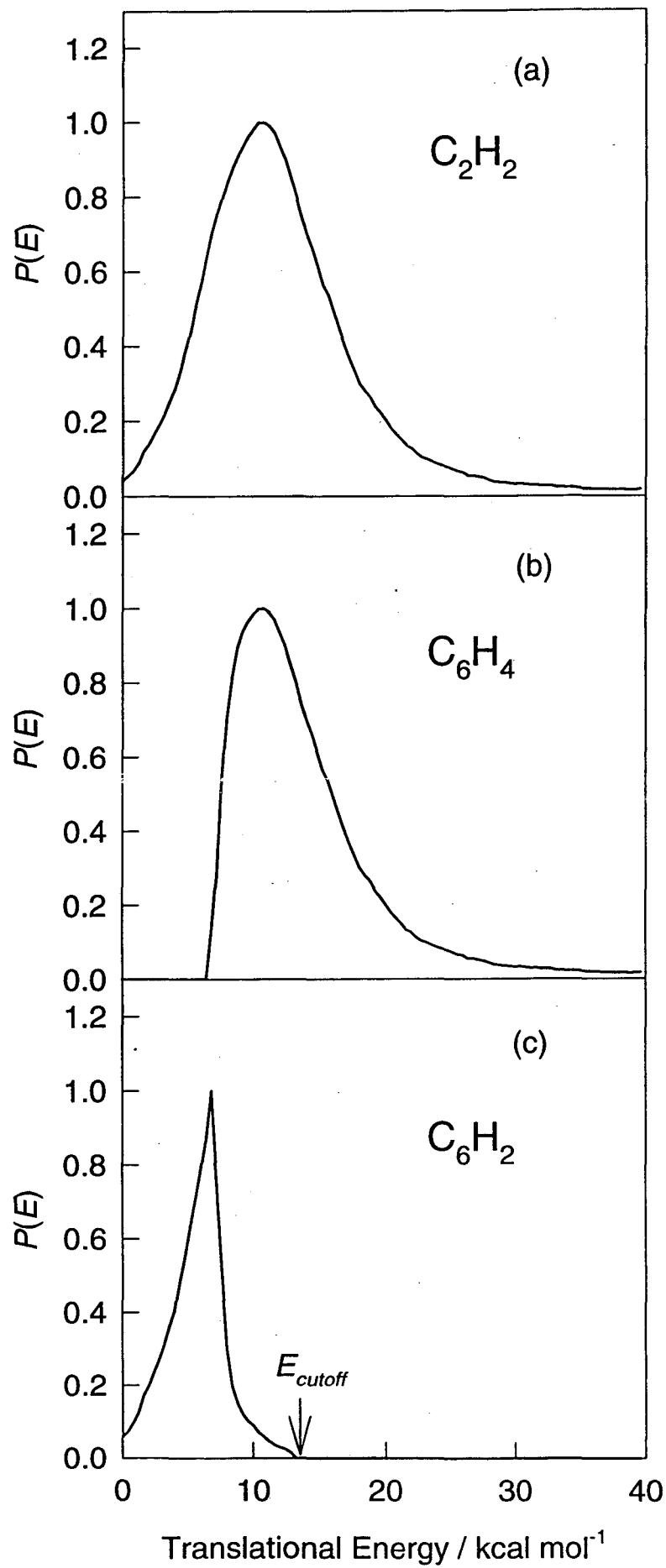
	Enthalpy of Formation, ΔH_f / kcal mol^{-1}		
	B3LYP/6-311G(d,p)	G2	Experiment
Acetylene	61.7	58.3	54.19[a]
1,3-butadiyne	115	109	111[b]
1,3,5-hexatriyne	171	161	160[c]

[a] Reference 62. [b] Reference 63. [c] Determined from the experimental data presented in this paper (refer to the text and Fig. 4).
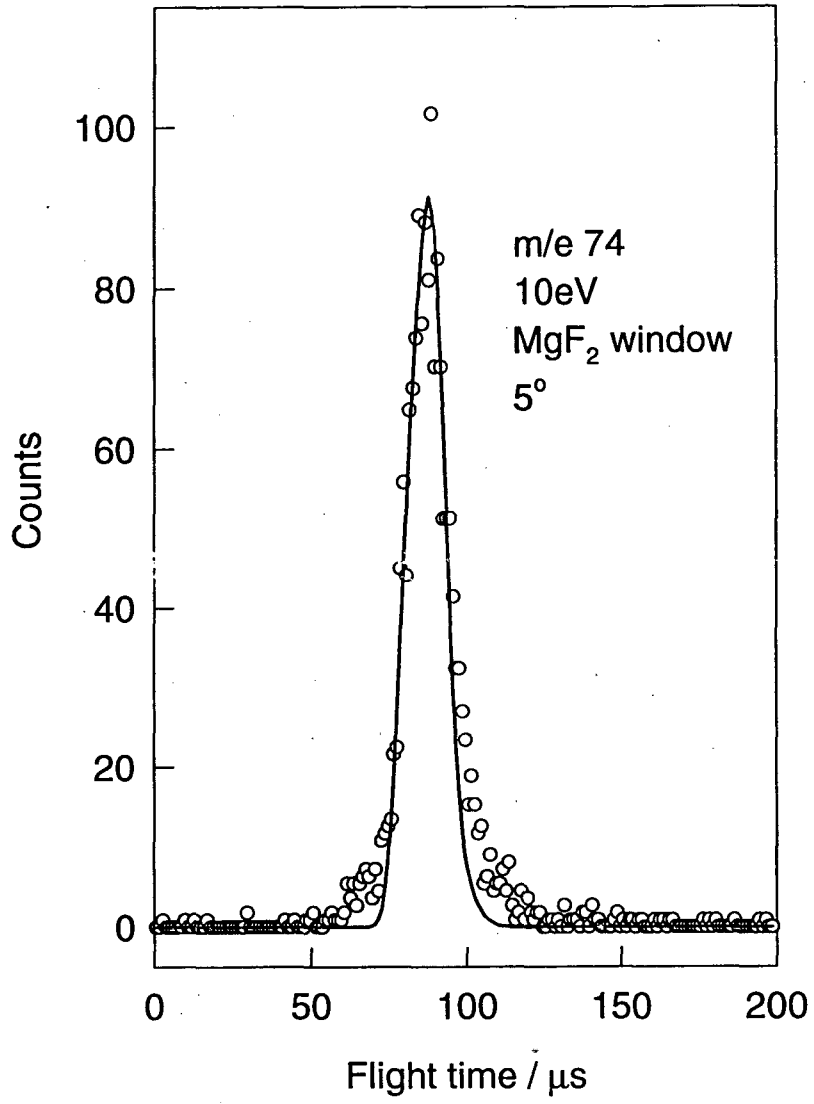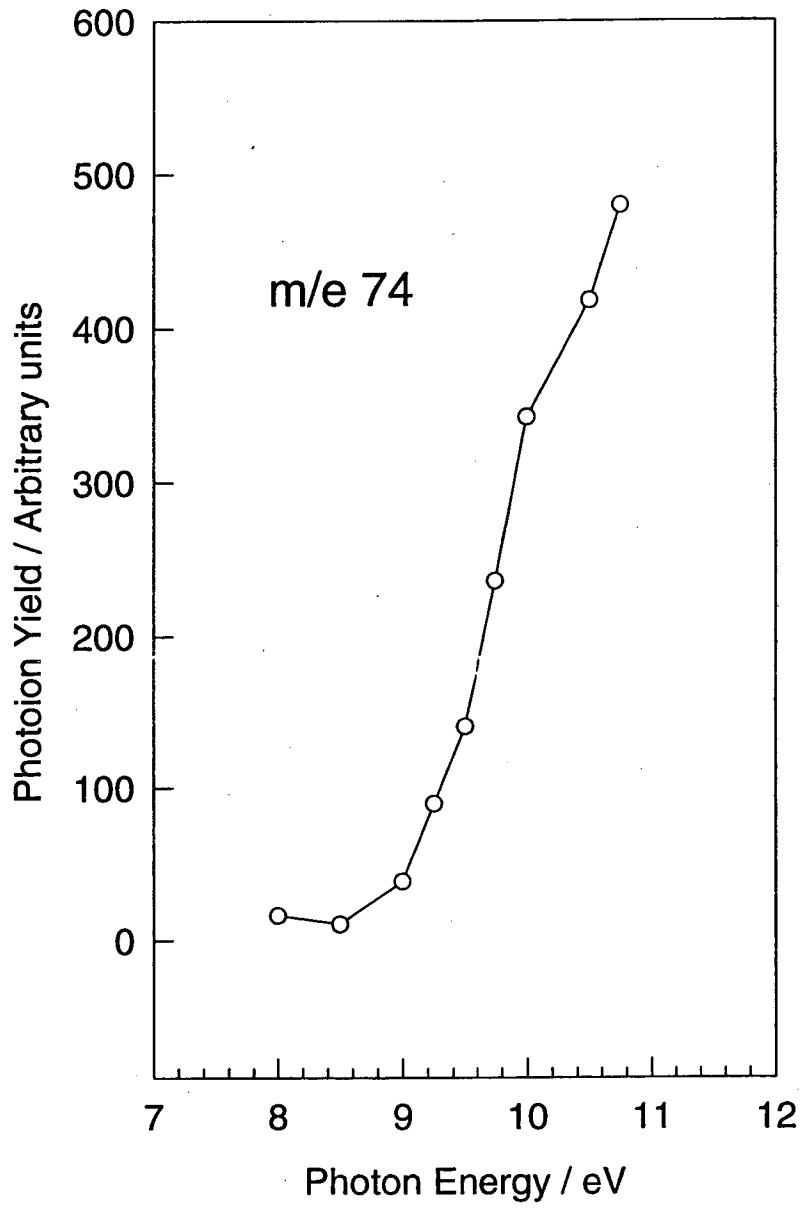
Fig. 1

FIG 2

m/e 76
10 eV, MgF$_2$ window
20°

m/e 76
10 eV, MgF$_2$ window
15°

m/e 76
10 eV, MgF$_2$ window
20°

Flight time / μs

F 11-3

Translational Energy / kcal mol⁻¹

FIG 4

m/e 74
10eV
MgF$_2$ window
5°

Flight time / μs

Counts

FIG 5

FIG 6